Supporting Information

Transition Metal Substituted Sandwich-Type Polyoxometalates with Strong Metal–C (imidazole) Bond as Anticancer Agents

Hongxia Zhao,[a] Li Tao,[b] Fengmin Zhang,[c] Ying Zhang,[a] Yanqing Liu,*[b] Hongjie Xu,[a] Guowang Diao,*[a] Lubin Ni*[a]

[a]School of Chemistry and Chemical Engineering, Yangzhou University, Yangzhou 225002, Jiangsu, People's Republic of China.

[b]College of Medicine, Yangzhou University, Yangzhou 225001, People's Republic of China.

[c]Testing Center, Yangzhou University, Yangzhou, 225002 Jiangsu, People's Republic of China

Table of Contents

Experimental Section

Materials and physical measurements. $[N(CH_3)_4]_{10}Na_{12}[Na_2Sb_8W_{36}O_{132}(H_2O)_4]$ $26H_2O$ **{Sb_8W_{36}}** as precursor material was prepared according to the previous literature.[S1] Other chemicals were commercially purchased and used without further purification. Elemental analyses (C, H, O and N) were performed using an EA 1110 elemental analyzer. Elemental analyses of metals (Na, W, Ni, Sb) were measured by ICP-OES on Optima 7300 DV (PerkinElmer). Fourier transform infrared (FT-IR) spectra were recorded on a Perkin-Elmer BXII spectrometer with KBr pellets. Raman spectroscopy was performed on a Renishaw Ramascope 1000 with a green SpectraPhysics Argon laser (wavelength of 524.5 nm and 50 mW capacity). UV/vis spectra were recorded on a Carry5000 UV/vis spectra. Fluorescence spectra were recorded using a Shimadzu RF-5301 spectrofluorophotometer from 290 to 500 nm at an excitation wavelength of 280 nm. Solid ^{13}C NMR spectra were recorded on a Bruker AV 400 NMR spectrometer using cross polarization, magic angle spinning (12 kHz) and hexamethylbenzene (HMB) as the reference. Solution ^{1}H NMR spectra were recorded on a Bruker Avance AV-400M Hz resonance spectrometer with D_2O solvent using DSS (sodium 2,2-dimethyl-2-silapentane-5-sulfonate) as an internal reference or $(CD_3)_2SO$ (DMSO-d6) solvent at room temperature. The thermogravimetric analyses (TGA) were performed with a Netzsch TG209 F1 instrument at 10 ℃ min^{-1} from 25 to 1000 ℃ in a flowing air atmosphere. X-ray powder diffraction (XRD) data were obtained with a graphite monochromator and Cu Kα radiation (λ= 0.1541 nm) on a D8 advance super speed powder diffractometer (Bruker). The XPS experiments were carried out on a Thermo Escalab 250 system using Al Kα radiation (hν = 1486.6 eV). The test chamber pressure was maintained below 2×10^{9} Torr during spectral acquisition. Cyclic voltammetry experiments were carried out with an electrochemical workstation (CHI660 E,

Chenghua, China). The three-electrode cell system consisted of a 2 mm glassy carbon working electrode (GCE, modified or unmodified), a saturated Ag/AgCl reference electrode and a Pt wire as the counter electrode.

Synthesis of $H[(CH_3)_4N]_4\{[Na(H_2O)_4][Na_{0.7}Ni_{5.3}(imi)_2(Himi)(H_2O)_2(SbW_9O_{33})_2]\}\cdot 10H_2O$ (1).

1.032 g (0.085 mmol) **$\{Sb_8W_{36}\}$** was dissolved in 20 mL of deionized water under stirring for 10 mins. Afterwards, 0.10 g (0.1 mmol) of $NiCl_2\ 6H_2O$ and mL of 1.2 M imidazole solution (0.5 mL) were added in individual portions with stirring for 0.5 h, followed by a color change to light yellow at pH values around 6.5. Next, an additional amount of 1.0 M NaOH solution (5.0 mL) was added to adjust the pH value at 7.6. The resulting mixture was kept at room temperature with slow evaporation for 2-4 days, resulting in orange blocklike crystals. (Yield:30.56 % based on **$\{Sb_8W_{36}\}$**). TGA showed a weight loss of 4.28 % in the 30–214 ℃ temperature range, corresponding to the loss of coordinating and solvent water molecules (expected 5.04 %). The second weight loss of 9.39% between 214 ℃ and 560 ℃ arises from the loss of three imidazole organic ligands and four peripheral countercations $[(CH_3)_4N]^+$ and Na^+. (expected 9.84%). Elemental analysis: found for compound **1** (calculated): C 5.67 (5.23), H 1.71 (1.69), O 23.53 (22.85), N 2.28(2.44), Ni 5.14 (5.11), W 60.54 (60.53), Na 0.66 (0.80), Sb 4.92 (4.24). FT-IR (KBr pellet, cm^{-1}): 3433 (m), 3045(m), 2856(w), 1605 (m), 1335 (m), 1184 (m), 1076 (w), 950 (s), 883 (s), 741 (m), 661 (s), 443 (m). Raman (cm^{-1}): 3166(m), 2987(m), 1452(m), 967 (s), 890(s), 827(s), 749(s).

Synthesis of $H_2[(CH_3)_4N]_4[Na_{0.7}Co_{5.3}(imi)_2(Himi)(H_2O)_2(SbW_9O_{33})_2]\cdot 12H_2O$ (2).

The synthetic procedure was conducted as described above for **1** with one alteration: instead of $NiCl_2\ 6H_2O$, 0.1 g (0.1 mmol) of $CoCl_2\ 6H_2O$ was added to the reaction mixture. 0.531 g of dark blue blocklike crystals were obtained after about 1 week (Yield: 47.44 % based on **$\{Sb_8W_{36}\}$**).

Elemental analysis: found for compound **2** (calculated): C 5.9 (5.25), H 1.98 (1.64), O 23.53 (22.95), N 2.66(2.45), Co 4.69 (5.15), W 56.7 (57.89), Na 0.34 (0.4), Sb 4.89 (4.26). TGA showed a weight loss of 4.41 % in the 25–220 ℃ temperature range, corresponding to the loss of coordinating and solvent water molecules (expected 3.19 %). The second weight loss of 9.22% between 220 ℃ and 688 ℃ arises from the loss of three coordinated imidazole organic ligands and four peripheral countercations $[(CH_3)_4N]^+$. (expected 8.75%). FT-IR (KBr pellet, cm^{-1}): 3449(m), 3030(m), 3147(m), 2844(w), 1637 (m), 1079 (m), 1076 (w), 942 (s), 877 (s), 732 (m), 667 (s), 449 (m). Raman (cm^{-1}): 3159(m), 3044(m), 2937(w), 2823(w), 1452(m), 965 (s), 887(s), 753(s).

X-ray crystallography. Crystal structure determinations by X-ray diffraction for compounds **1** and **2** were performed on a Bruker SMART APEX II CCD diffractometer with graphite-monochromated (MoK_α radiation, λ = 0.71073 Å) at room temperature. The structure was solved by direct method [S2-S3] (SHELXTL-2014/7 and Olex1.2) and refined by full-matrix-block least squares methods on F^2. All calculations were performed using the SHELXTL-2014/7 program package. Hydrogen atoms were not included in the refinements and heavy metal atoms (Sb, Ni, W and Na) were refined anisotropically. Hydrogen atoms of crystalline water molecules were omitted. Further details of the X-ray structural analysis are given in Table S1. Selected bond lengths are listed in Table S2-S3.

Cell culture. Human hepatocellular carcinoma (HCC) cell lines HepG2 and SMMC-7721 were purchased from the Cell Bank of the Chinese Academy of Sciences (Shanghai, P. R. China). Human non-small cell lung cancer (NSCLC) H1299 and A549, human gastric carcinoma cell lines AGS and BGC-823 and human embryonic kidney 293T cells were all obtained from the American Type

Culture Collection (ATCC, Rockville, MD). HepG2, SMMC-7721 and 293T cells were cultured in Dulbecco's Modiified Eagle's Medium (DMEM) containing 10% fetal bovine serum (FBS, Gibco) and 1% penicillin–streptomycin solution. H1299, A549, AGS and BGC-823 cells were grown and maintained in RPMI-1640 medium with 10% FBS. All cells were maintained at a humidiified atmosphere containing 5% CO_2 at 37 ℃.

***In Vitro* Cytotoxicity Assay.** The cytotoxicity of compound **1** against a panel of tumor cells including HepG2, SMMC-7721, H1299, A549, AGS and BGC-823 was assessed by MTT assay, while HEK293T was used as a non-neoplastic cell control. Cisplatin served as positive treatment control. Cells were seeded in 96-well cell culture plate at a density of 3×10^3 cells per well and treated with different concentrations of Compound **1** for 48 h, and subsequently incubated with 20 μL/well of 0.5 mg/mL MTT solution. After additional incubation of 4 h, the medium was carefully aspirated and replaced with 150 μL/well of DMSO. After brief shaking for 15 min, the absorbance was measured with Enspire™Multilabel Plate Reader (PerkinElmer) at 480 nm. IC_{50} (half-maximal inhibitory concentration) values were calculated by probit analysis using SPSS software program. The curves of cell viability of compound **1** treatment were drawn in comparison with control group. The inhibitory rate was calculated using the following equation: inhibitory rate (%) = $(OD_{control} - OD_{treatment})/OD_{control} \times 100\%$.

Flow cytometric analysis. To measure cell cycle distribution upon compound **1** exposure, AGS and BGC-823 cells treated with compound **1** for 24 h were collected, washed with PBS, fixed with 75% ethanol at 4 ℃ overnight and treated with RNase A for 30 min, followed by PI staining for 30 min. The alteration of the cell cycle was analyzed by FACSAria SORP flow cytometer. For apoptosis detection, AGS and BGC-823 cells were treated with compound **1** under 40 μM and 120 μM

respectively for 24 h. Apoptotic cells were determined using a Fluorescein isothiocyanate (FITC)-labeled annexinV (Annexin-V-FITC)/PI apoptosis staining kit according to the manufacturer's instructions. Fresh cells were collected and resuspended in 500 μL of binding buffer, stained with 5 μL of Annexin-V-FITC and 5 μL of PI. Finally, the samples were analyzed with the FACSAria SORP flow cytometer.

Nuclear morphology. All cells were seeded on 10 mm^2 glass coverslips placed in 6-well plates at a density of 1 $\times 10^5$ cells/well and allowed to grow for 24 h. Then, AGS cells and BGC-823 cells were treated with compound **1** (0, 5, 20 μM, respectively) for 24 h at 37 ℃, respectively. Subsequently, cells washed one time with PBS, fixed with 4% paraformaldehyde solution for 15 min at room temperature, then washed three times with PBS and stained with Hoechst33258 for 15 min at room temperature, then washed two times with PBS and nuclear morphology was observed under Fluorescence microscopy and images were taken at a magnification of 200×.

Binding nature of BSA with compounds

BSA solution (2 μM) in Tris (pH =7.4) was titrated with compound **1**, imi and **{SbW_9}** for 2.5 μM. After equilibration, absorption spectra measurements were carried out on a Carry5000 UV/vis spectrophotometer at 200–500 nm. Fluorescence spectra were recorded using a Shimadzu RF-5301 spectrofluorophotometer from 290 to 500 nm at an excitation wavelength of 280 nm. BSA solution (2 μM) in Tris (pH = 7.4) was titrated with compound **1**, imi and **{SbW_9}** form 1–10 μM in 298K and 318K.

References

[S1] Michael Bosing, h a Loose, Heinrich Pohlmann and Bernt Krebs, *Chem. Eur. J.*, 1997, 3, No. 8.
[S2] G. M. Sheldrick. SHELXTL Version 2014/7. http://shelx.uni-ac.gwdg.de/SHELX/index.php.
[S3] O. V. Dolomanov, L. J. Bourhis, R. J. Gildea, J. A. K. Howard, H. Pitchman, J. Appl. Cryst., 2009, 42, 339

Table S1. Crystallographic data for the Compounds 1 and 2.

Compound	Compound **1**	Compound **2**
Formula	$C_{25}N_{10}Na_{1.7}Ni_{5.3}O_{82}Sb_2W_{18}$	$C_{25}N_{10}Na_{0.7}Co_{5.3}O_{76}Sb_2W_{18}$
FW, $g.mol^{-1}$	5655.40	5537.57
T, K	298(K)	298(K)
crystal size (mm)	0.16 × 0.12 × 0.09	0.21 × 0.11 × 0.06
crystal system	Monoclinic	Monoclinic
space group	C2/c	C2/c
a, Å	22.4271(14)	22.354(4)
b, Å	22.3391(14)	22.392(5)
c, Å	25.7151(15)	25.922(5)
V, $Å^3$	11768.2(13)	11836(4)
Z	4	4
ρ_{calc}, $g.cm^{-3}$	3.129	3.108
λ(Mo K), Å	0.71073	0.71073
θrange, deg	θ_{max} = 27.103 °, θ_{min} = 1.809 °	θ_{max} = 27.101 °, θ_{min} = 1.809 °
data collected	55150	53613
unique data	12881	12999
no. Parameters	589	403
restraints	20	31
GOF	1.065	1.028
R_{int}	0.0380	0.0930
$R_1[I > 2\ (I)]$	0.0517	0.0833
wR_2 indices $[I > 2\ (I)]$	0.1123	0.1886

$R_1 = \sum(Fo - Fc)/\sum Fo$ and $wR_2 = \{\sum w(Fo^2 - Fc^2)^2/\sum w(Fo^2)^2\}^{1/2}$

Table S2. Selected Bond lengths [Å] for compound 1.

W(1)-O(1)	1.725(11)	W(1)-O(2)	1.904(11)	W(1)-O(3)	1.904(12)
W(1)-O(4)	1.926(11)	W(1)-O(5)	1.950(12)	W(1)-O(11)	2.319(8)
W(2)-O(10)	1.716(11)	W(2)-O(5)	1.886(12)	W(2)-O(9)	1.915(11)
W(2)-O(7)	1.935(13)	W(2)-O(6)	1.941(12)	W(2)-O(8)	2.291(8)
W(3)-O(36)	1.728(11)	W(3)-O(4)	1.891(12)	W(3)-O(14)	1.905(12)
W(3)-O(13)	1.910(12)	W(3)-O(9)	1.935(11)	W(3)-O(12)	2.324(8)
W(4)-O(17)	1.711(9)	W(4)-O(16)	1.882(9)	W(4)-O(24)	1.887(8)
W(4)-O(13)	1.956(10)	W(4)-O(18)	1.967(9)	W(4)-O(12)	2.285(8)
W(5)-O(19)	1.718(9)	W(5)-O(23)	1.881(9)	W(5)-O(20)	1.912(9)
W(5)-O(18)	1.946(9)	W(5)-O(14)	1.953(11)	W(5)-O(12)	2.282(8)
W(6)-O(21)	1.716(10)	W(6)-O(22)	1.852(9)	W(6)-O(20)	1.929(9)
W(6)-O(33)#1	1.945(9)	W(6)-O(7)	1.954(11)	W(6)-O(8)	2.287(9)
W(7)-O(28)	1.714(10)	W(7)-O(27)	1.824(8)	W(7)-O(29)	1.937(8)
W(7)-O(16)#1	1.944(9)	W(7)-O(3)#1	1.980(10)	W(7)-O(11)#1	2.303(8)
W(8)-O(30)	1.726(9)	W(8)-O(25)	1.819(8)	W(8)-O(31)	1.923(9)
W(8)-O(29)	1.945(9)	W(8)-O(2)#1	2.000(10)	W(8)-O(11)#1	2.274(8)
W(9)-O(32)	1.721(10)	W(9)-O(26)	1.858(9)	W(9)-O(31)	1.909(10)
W(9)-O(33)	1.941(9)	W(9)-O(6)#1	1.964(11)	W(9)-O(8)#1	2.310(8)
Sb(1)-O(8)	2.000(9)	Sb(1)-O(12)	2.004(8)	Sb(1)-O(11)	2.014(9)
Sb(2)-O(11)	1.833(11)	Sb(2)-O(12)	1.857(11)	Sb(2)-O(8)	1.858(12)
Ni(1)-C(4)	1.969(16)	Ni(1)-O(23)#1	1.989(8)	Ni(1)-O(23)	1.989(8)
Ni(1)-O(22)	2.005(8)	Ni(1)-O(22)#1	2.005(8)	Ni(2)-O(24)	2.191(8)
Ni(2)-O(23)	2.196(9)	Ni(2)-O(26)	2.240(9)	Ni(2)-O(22)#1	2.249(9)
Ni(2)-O(37)	2.40(2)	Ni(3)-O(27)#1	1.982(8)	Ni(3)-O(25)	1.991(8)
Ni(3)-O(24)	2.010(8)	Ni(3)-O(26)	2.016(8)	Ni(3)-N(1)	2.001(9)
Ni(4)-O(27)	2.278(9)	Ni(4)-O(25)	2.293(9)	Ni(4)-O(25)#1	2.293(9)
Ni(4)-O(27)#1	2.278(9)				
Na(1)-O(34A)	1.74(4)	Na(1)-O(34)	2.21(3)	Na(1)-O(10)	2.35(2)
Na(1)-O(35)	2.75(3)	Na(1)-O(35A)	2.38(5)	Na(2)-O(27)	2.278(9)
Na(2)-O(27) #1	2.278(9)	Na(2)-O(25)	2.293(9)	Na(2)-O(25) #1	2.293(9)
Na(2)-O(29)	2.986(9)	Na(2)-O(29) #1	2.986(9)		
N(1)-C(1)	1.305(16)	N(1)-C(3)	1.357(16)	N(2)-C(1)	1.313(18)
N(2)-C(2)	1.35(2)	N(3)-C(4)	1.37(2)	N(3)-C(5)	1.38(2)
C(2)-C(3)	1.36(2)	C(4)-N(3)#1	1.37(2)	C(5)-C(5)#1	1.31(4)
N(4)-C(9)	1.49(4)	N(4)-C(7)	1.55(3)	N(4)-C(6)	1.56(3)
N(4)-C(8)	1.66(4)	N(5)-C(12)	1.49(4)	N(5)-C(14)	1.57(4)
N(5)-C(11)	1.57(3)	N(5)-C(13)	1.62(4)		

Symmetry transformations: #1 -x+1, y, -z+1/2

Table S3. Selected Bond lengths [Å] for compound 2.

W(1)-O(3)	1.71(2)	W(1)-O(6)	1.84(5)	W(1)-O(9)	1.887(19)
W(1)-O(10)	1.899(19)	W(1)-O(4)	1.892(18)	W(1)-O(13)	2.312(15)
W(2)-O(2)	1.79(2)	W(2)-O(7)	1.90(2)	W(2)-O(5)	1.913(19)
W(2)-O(8)	1.944(19)	W(2)-O(6)	1.98(5)	W(2)-O(14)	2.309(14)
W(3)-O(1)	1.71(3)	W(3)-O(12)	1.85(2)	W(3)-O(11)	1.890(19)
W(3)-O(5)	1.904(19)	W(3)-O(4)	1.905(18)	W(3)-O(15)	2.347(16)
W(4)-O(22)	1.71(2)	W(4)-O(32)	1.859(18)	W(4)-O(16)	1.932(18)
W(4)-O(21)	1.942(17)	W(4)-O(8)	1.943(19)	W(4)-O(14)	2.304(14)
W(5)-O(26)	1.75(2)	W(5)-O(31)	1.850(17)	W(5)-O(21)	1.939(18)
W(5)-O(34)	1.964(19)	W(5)-O(7)	2.01(2)	W(5)-O(14)	2.289(14)
W(6)-O(20)	1.70(2)	W(6)-O(30)	1.863(17)	W(6)-O(34)	1.876(19)
W(6)-O(19)	1.964(17)	W(6)-O(12)	2.03(2)	W(6)-O(15)	2.295(16)
W(7)-O(25)	1.70(2)	W(7)-O(29)	1.800(17)	W(7)-O(19)	1.927(17)
W(7)-O(18)	1.946(18)	W(7)-O(11)	1.973(19)	W(7)-O(15)	2.319(16)
W(8)-O(24)	1.692(19)	W(8)-O(28)	1.853(16)	W(8)-O(18)	1.892(19)
W(8)-O(17)	1.949(16)	W(8)-O(10)	1.981(19)	W(8)-O(13)	2.278(15)
W(9)-O(23)	1.715(18)	W(9)-O(27)	1.860(18)	W(9)-O(16)	1.921(18)
W(9)-O(9)	1.970(19)	W(9)-O(17)	1.960(15)	W(9)-O(13)	2.309(15)
Sb(1)-O(15)	2.000(17)	Sb(1)-O(14)	2.028(14)	Sb(1)-O(13)	2.048(15)
Co(1)-O(29) #1	2.289(17)	Co(1)-O(29)	2.289(17)	Co(1)-O(30)#1	2.297(17)
Co(1)-O(30)	2.297(17)	Co(2)-O(27)	2.021(18)	Co(2)-O(27)#1	2.021(18)
Co(2)-O(32)#1	2.039(18)	Co(2)-O(32)	2.039(18)	Co(2)-C(4)	2.04(3)
Co(3)-O(27)	2.218(18)	Co(3)-O(28)	2.228(17)	Co(3)-O(32)#1	2.232(18)
Co(3)-O(31)#1	2.263(17)	Co(3)-O(33)	2.38(4)	Co(4)-O(30)	1.957(17)
Co(4)-N(1)	2.02(2)	Co(4)-O(29)#1	2.037(17)	Co(4)-O(31)	2.042(17)
Co(4)-O(28)#1	2.059(17)				
Na(1)-O(29)#1	2.289(17)	Na(1)-O(29)	2.289(17)	Na(1)-O(30)#1	2.297(17)
Na(1)-O(30)	2.297(17)				
N(1)-C(1)	1.37(3)	N(1)-C(3)	1.37(3)	N(2)-C(1)	1.30(4)
N(2)-C(2)	1.31(5)	N(3)-C(5)#1	1.37(5)	N(3)-C(4)	1.38(5)
N(4)-C(7)	1.52(4)	N(4)-C(8)	1.56(4)	N(4)-C(6)	1.58(4)
N(4)-C(9)	1.66(6)	N(5)-C(11)	1.53(4)	N(5)-C(10)	1.55(4)
N(5)-C(12)	1.56(4)	N(5)-C(13)	1.65(6)	C(5)-N(3)#1	1.37(5)
C(2)-C(3)	1.52(5)	C(4)-N(3)#1	1.37(5)	C(5)-C(5)#1	1.31(9)

Symmetry transformations: #1 -x+1, y, -z+3/2

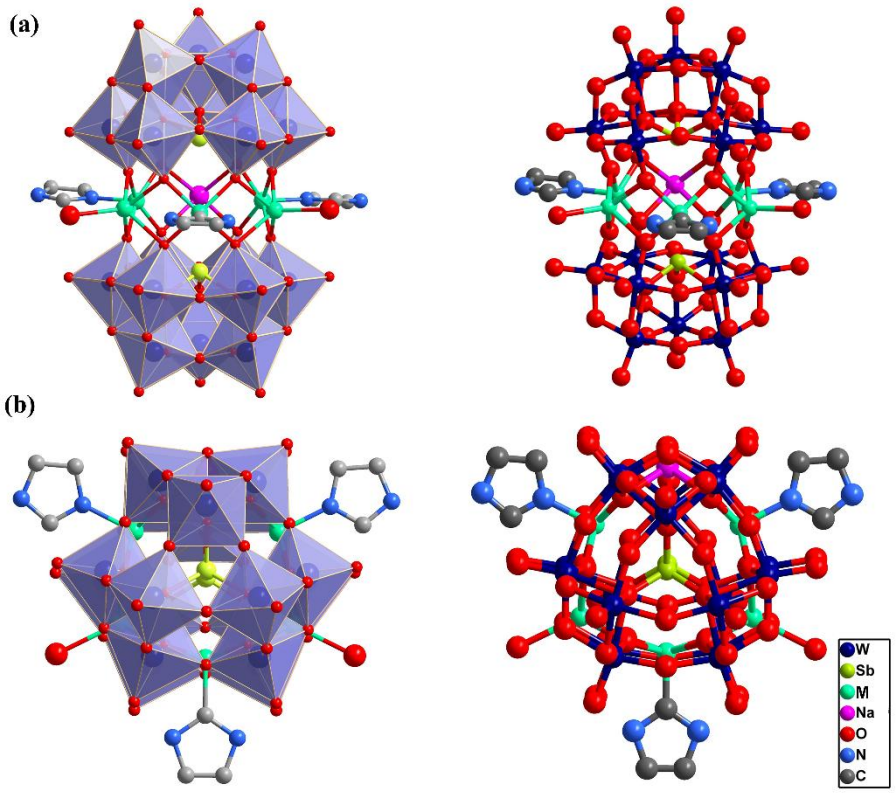

Figure S1. Polyhedral and ball-and-stick representation (a) front and (b) top views of the crystal structure of compounds **1** and **2** (M=Ni, Co). The cations and crystal water molecules are omitted for clarity. Only the major position of the disordered Na (0.7 occupancy) is shown for clarity.

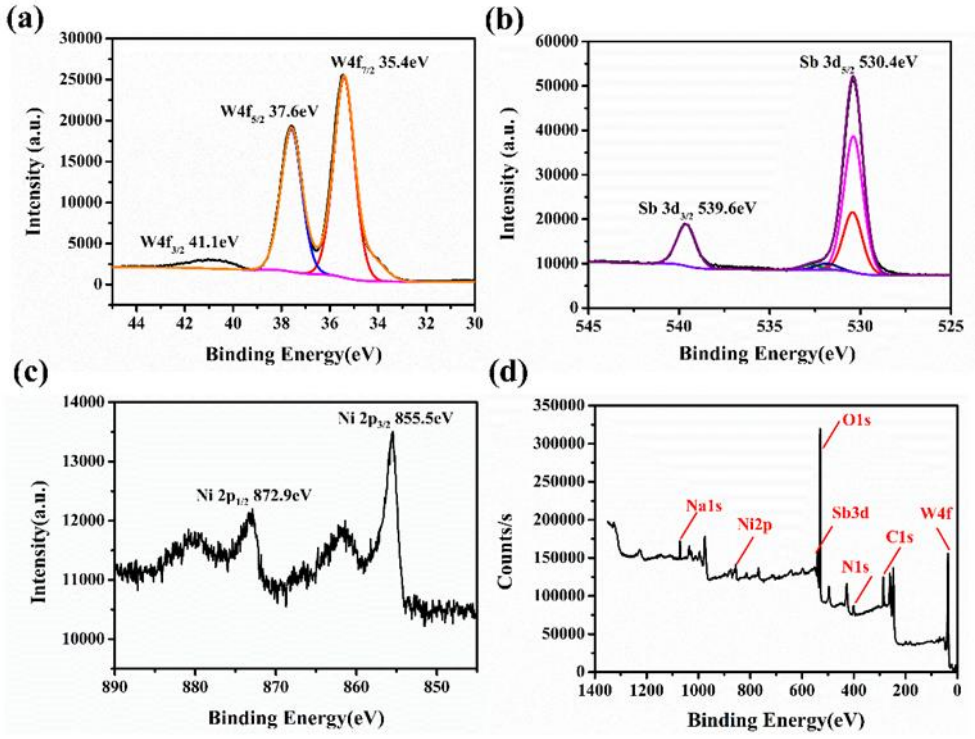

Figure S2. XPS spectrum of compound **1**, (a) for W, (b) for Sb, (c) for Ni and (d) for full spectrum.

Table S4. The binding energy for $W4f_{7/2}$, $W4f_{5/2}$, $Ni2p_{1/2}$, $Ni2p_{3/2}$ and $Sb3d_{3/2}$.

	Energy Region	Binding Energy(eV)
W^{6+}	$W4f_{7/2}$	34.8 eV
	$W4f_{5/2}$	37.2 eV
Ni^{2+}	$Ni2p_{1/2}$	855.5 eV
	$Ni2p_{3/2}$	872.9 eV
Sb^{3+}	$Sb3d_{3/2}$	539.6 eV

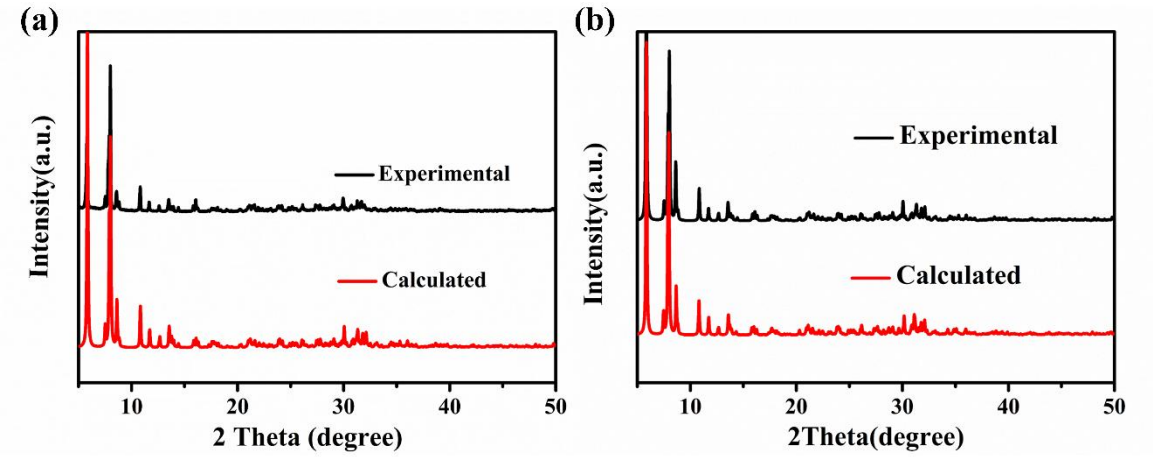

Figure S3. Calculated and experimental PXRD patterns of (a) compound **1** and (b) compound **2**.

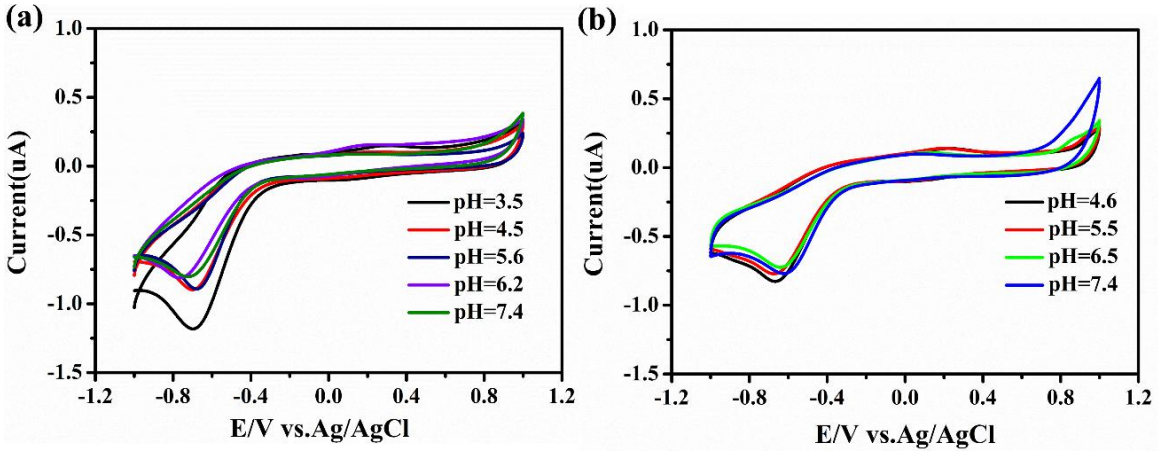

Figure S4. Cyclic voltammograms of 0.1 mM compounds **1** (a) and **2** (b) in (0.5 M CH_3COONa/CH_3COOH) buffer solution. (Scan rate 50 mV/s, GCE working electrode, Ag/AgCl reference electrode).

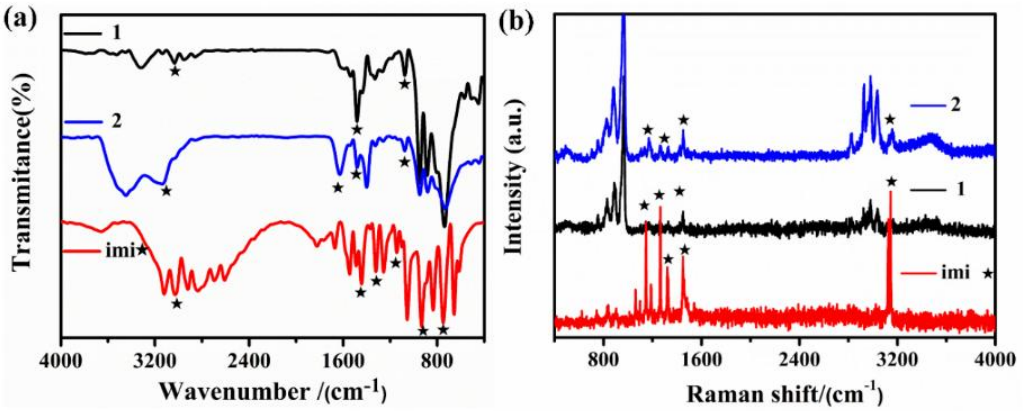

Figure S5. FT-IR (a) and Raman (b) spectra of compounds **1**, **2** and free imidazole ligand in the solid state.

Table S5. Vibrational features (IR and Raman) for compounds **1** and **2**.

		ν_{as}(W–Ot)	ν_{as}(W-O_b)	ν_{as}(W-O_c)	ν(C=C-H)	ν(C=C)	δ (CH_3, C-H)
1	IR	949	885	731	3045	1605	2955, 2856
	Raman	966	891	755	3116	1452	2980, 2816
2	IR	942	877	732	3030	1637	2962, 2846
	Raman	965	887	753	3044	1444	2973, 2830

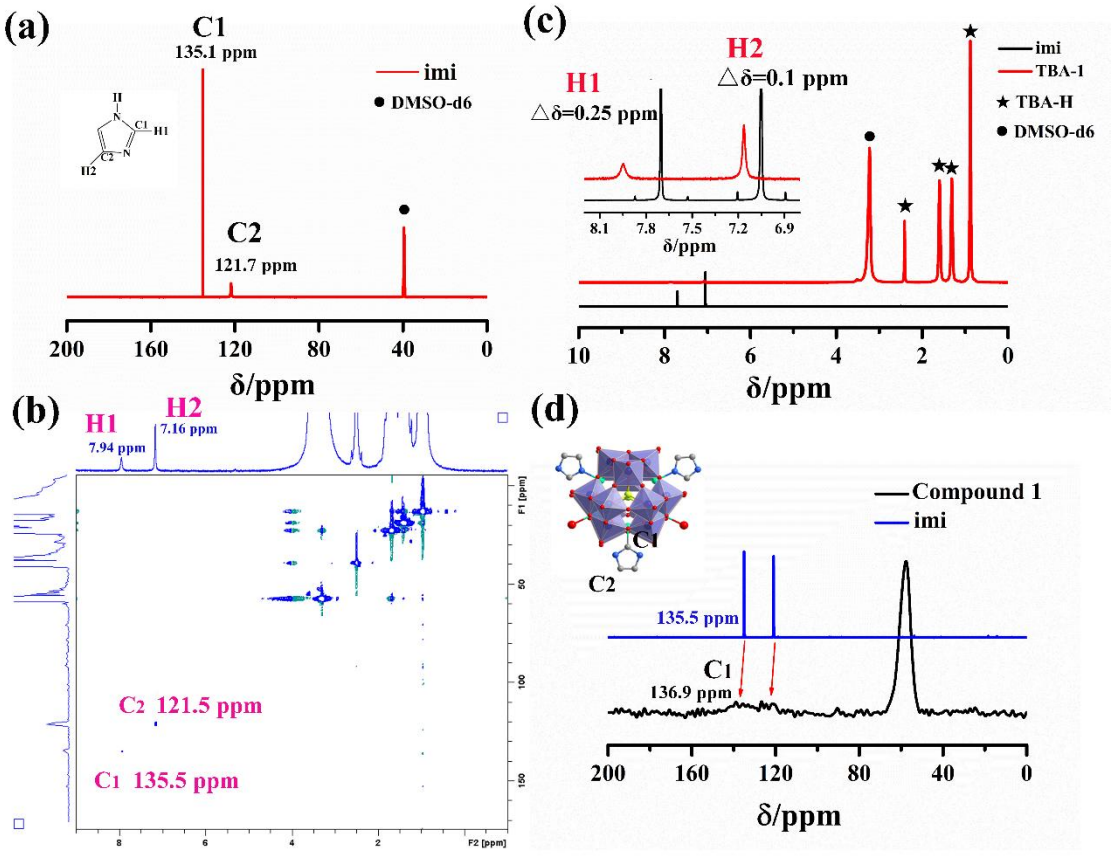

Figure S6. (a)^{13}C NMR spectrum of imidazole, (b) 2D ^{1}H–^{13}C heteronuclear single quantum coherence (HSQC) nuclear magnetic resonance (NMR) spectrum of tetrabutyl ammonium bromide-POM **1** (TBA-1), (c) ^{1}H NMR spectrum of imidazole and TBA-**1** in $(CD_3)_2SO$; (d) Solid ^{13}C NMR spectra of **1**.

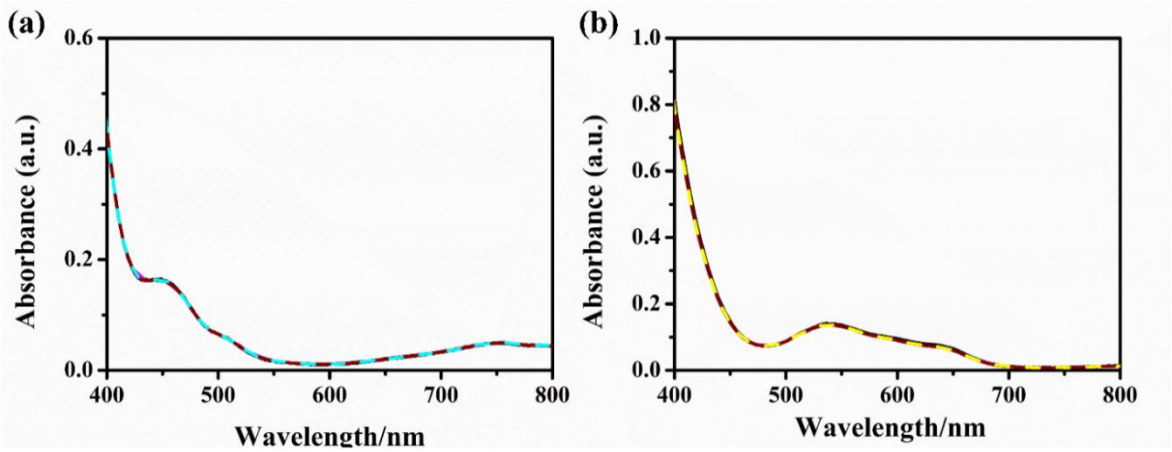

Figure S7. The UV-Vis spectra of (a) **1** and (b) **2**.

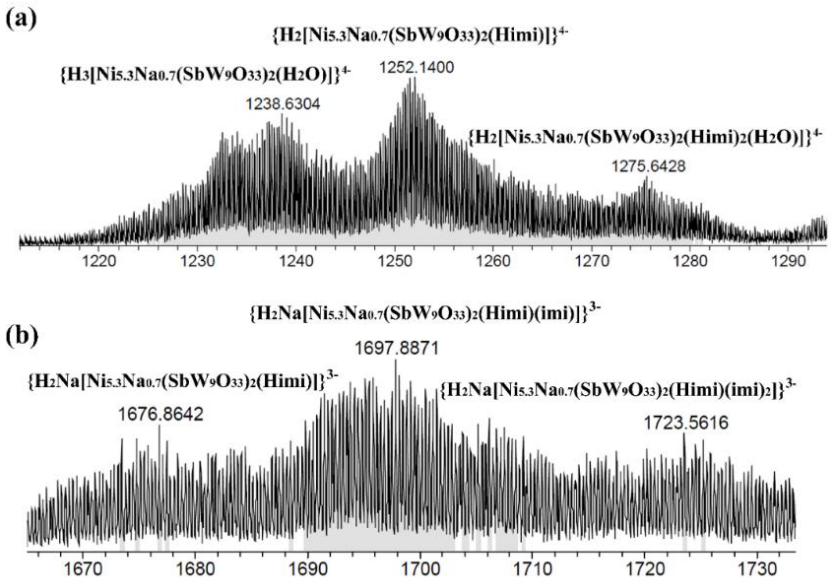

Figure S8. Negative ion electrospray ionization mass spectra (ESI-MS) of **1**.

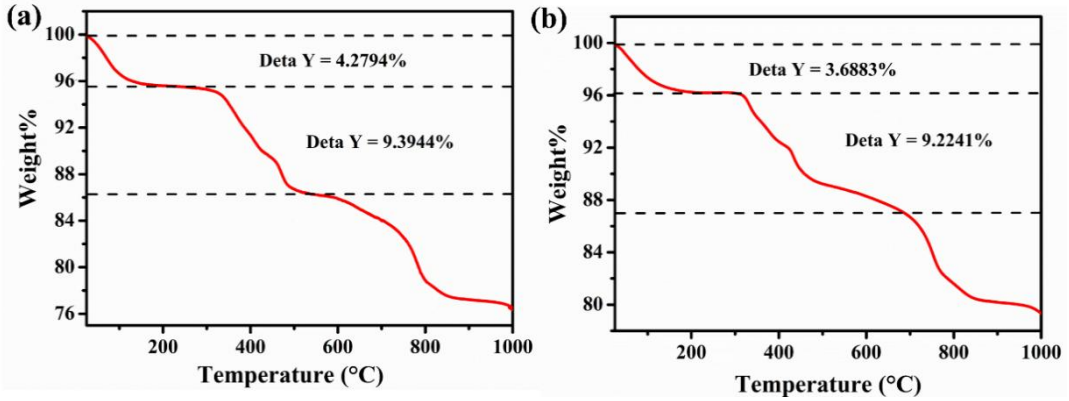

Figure S9. The thermal gravimetric analysis of (a) **1** and (b) **2**.

Table S6. IC_{50} values (μM) of compound **1** against HepG2, SMMC-7721, H1299, A549, AGS, BGC-823 and HEK293T after 48 h incubation, as determined by the MTT assay. Data are expressed as means ± SEM. (n= 3)

Cell lines		IC_{50} (μM)
Heptoma cells	HepG2	42.977 ± 0.47
	SMMC-7721	48.286 ± 0.32
Lung cancer cells	A549	39.72 ± 0.67
	H1299	63.23 ± 0.57
Gastric cancer cells	AGS	1.75 ± 0.58
	BGC-823	22.57 ± 0.47
Human embryonic kidney epithelial cells	HEK293T	114.76 ± 0.98

Table S7. IC_{50} values (μM) of compounds **1** and **2** against AGS, BGC-823 and HEK293T after a 48-hour incubation, as determined by the MTT assay. Data are expressed as means ± S.D. (n = 3)

	AGS	BGC-823	HEK293T
Compound 1	1.74 ± 0.58	22.57 ± 0.47	114.76 ± 0.98
Compound 2	1.42 ± 0.28	20.51 ± 1.39	103.09 ± 0.57
$\{Sb_8W_{36}\}$	2.86 ± 0.23	8.68 ± 0.66	
$\{SbW_9\}$	26.22 ± 2.21	188.28 ± 1.72	
Imi	>400	>400	
Cisplatin	17.44 ± 0.78	5.78 ± 0.25	

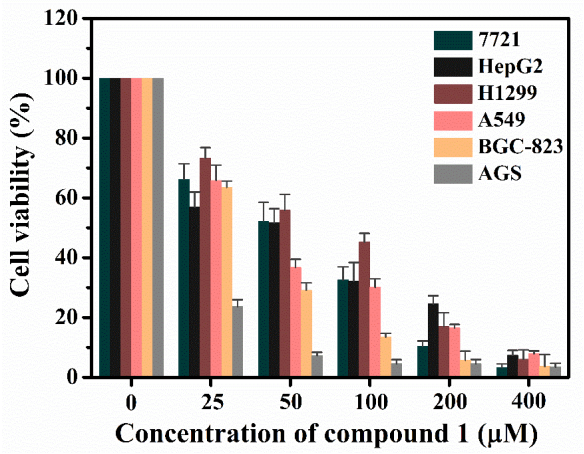

Figure S10. Cytotoxicity of compound **1** against human liver carcinoma cell lines 7721 and HepG2, lung carcinoma cells lines H1299 and A549, gastric carcinoma cell lines BGC-823 and AGS cells, as determined by the MTT assay after incubation for 48 hours.

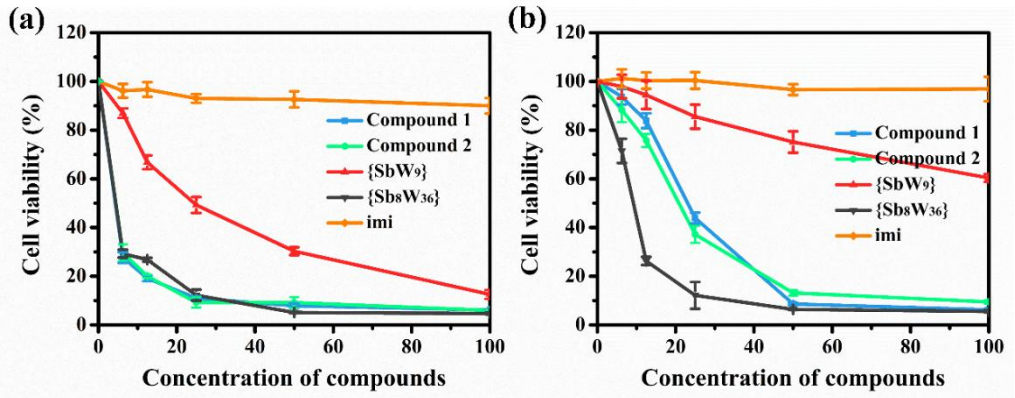

Figure S11. Cytotoxicity of two compounds, imidazole, **$\{Sb_8W_{36}\}$** and **$\{SbW_9\}$** against gastric carcinoma cell lines (a) AGS and (b) BGC-823 cells, as determined by the MTT assay after incubation for 48 hours. The results are presented as the means ± SD. of three independent experiments.

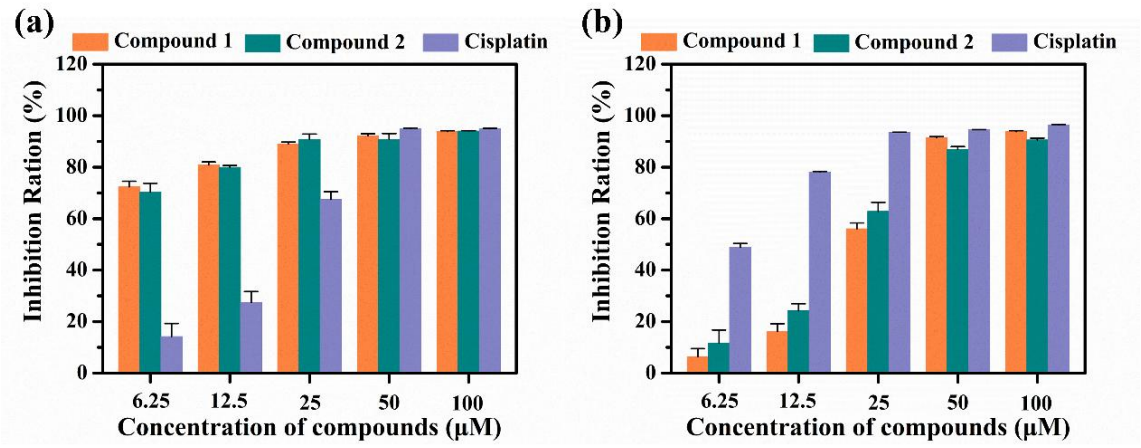

Figure S12. Two compounds and cisplatin inhibited the proliferation of gastric carcinoma cell lines (a) AGS and (b) BGC-823 cells, as determined by the MTT assay after incubation for 48 hours. The results are presented as the means ± SD. of three independent experiments.

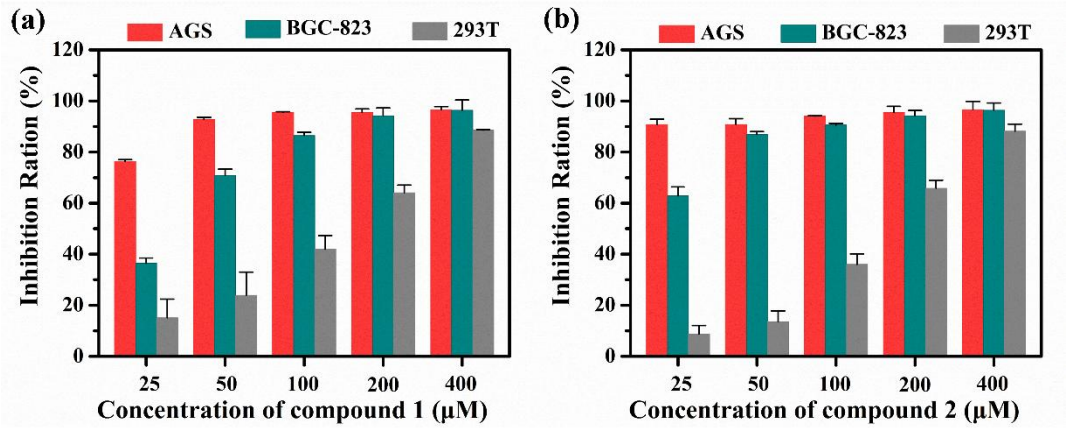

Figure S13. Inhibitory effect of compound **1** (a) and **2** (b) on AGS, BGC-823 and HEK293T cells after 48 h (n = 3, error bar = S.D.).

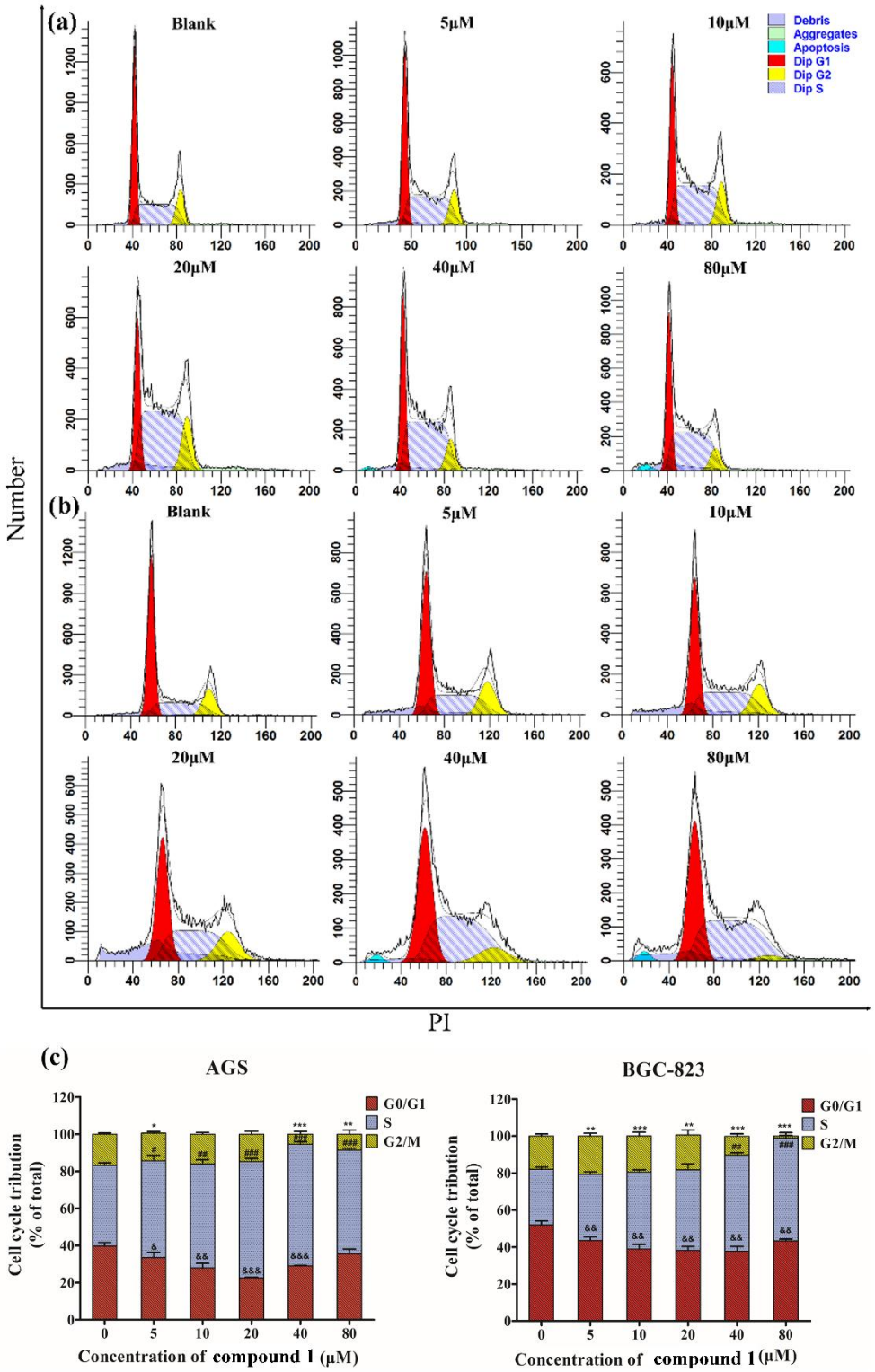

Figure S14. Compound **1** affected cell cycle distribution of (a) AGS and (b) BGC-823 cells. (c) Graphs depict the cell distribution in the different phases of the cell cycle determined by flow cytometry, and bar charts present the percentage of cells in the indicated phase of cell cycle. The results are presented as the means ± SD. of three independent experiments. P values were based on the Student's test: &&&< 0.001 compared with the control group at the G_0/G_1 phase; ###p < 0.001 compared with the control group at the S phase; *p < 0.05, **p < 0.01, ***p < 0.001 compared with the control group at the G_2/M phase.

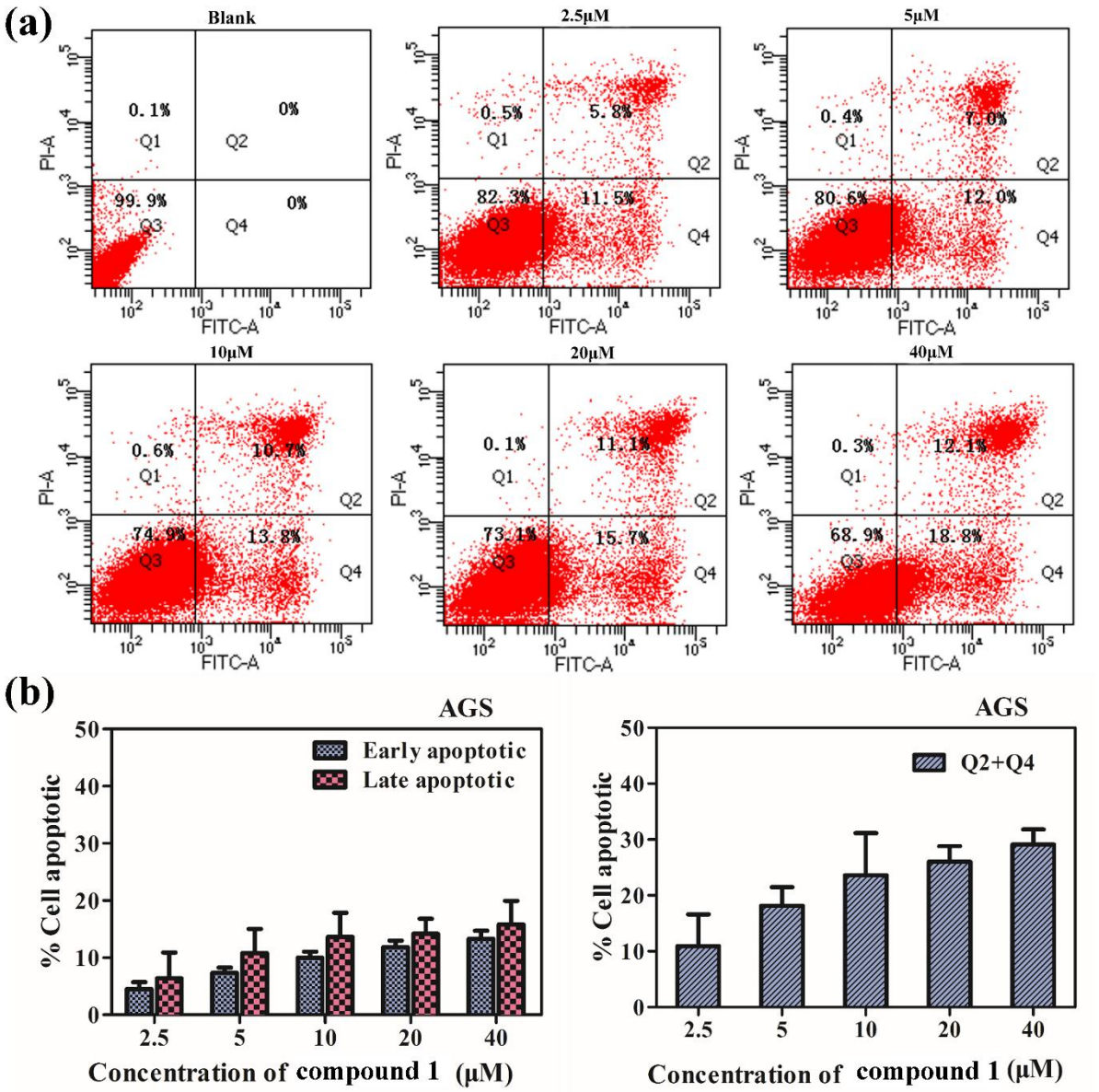

Figure S15. Annexin V/PI analysis of apoptosis in AGS cells; the lower-right panel presents early apoptotic cells, whereas the upper-right panel displays late apoptotic cells. The quantitative analysis of apoptosis induced in AGS treated with 0, 2.5, 5, 10, 20 and 40 μM of compound **1** for 24 h.

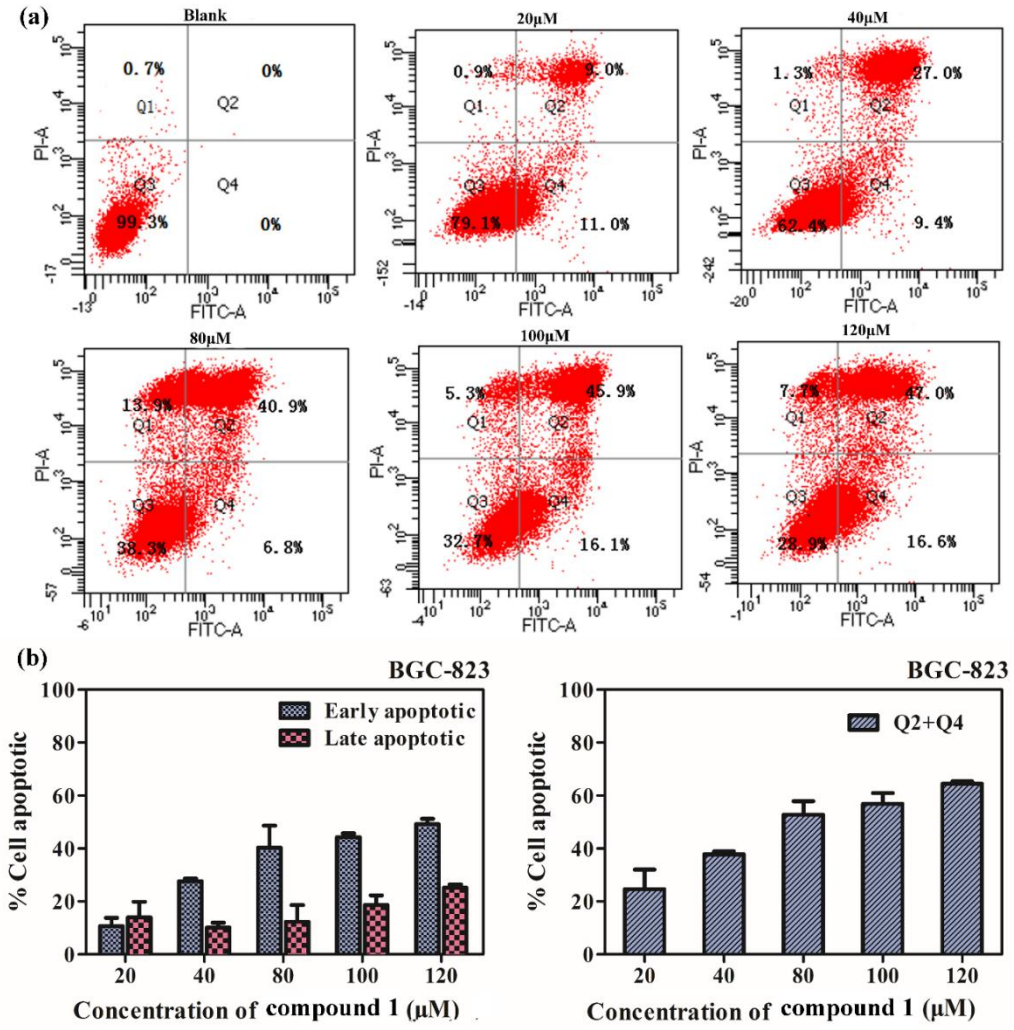

Figure S16. Annexin V/PI analysis of apoptosis in BGC-823 cells; The quantitative analysis of apoptosis induced in AGS treated with 0, 20, 40, 80, 100 and 120 μM of compound **1** for 24 h.

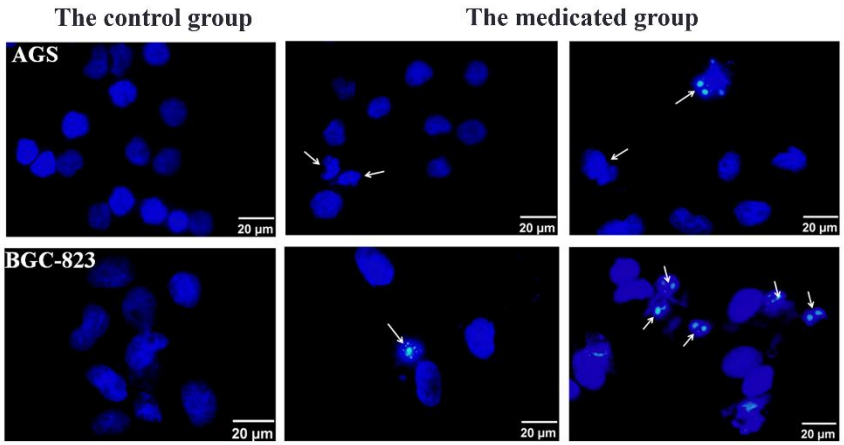

Figure S17. Morphological changes in AGS and BGC-823 cells treated with various concentrations of **1** for 24 h, which had been stained with Hoechst 33258 and detected by fluorescence microscope.

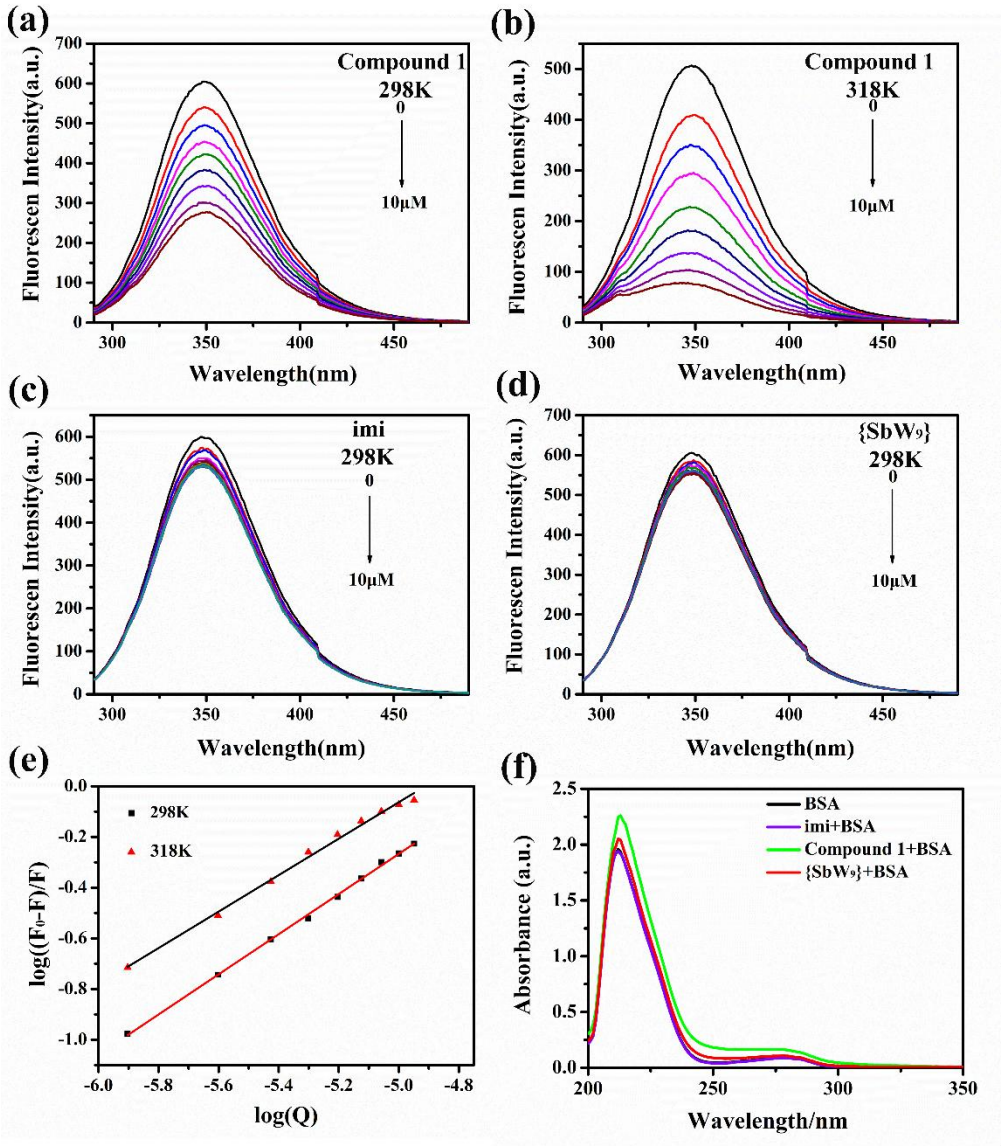

Figure S18. The fluorescence spectra of BSA in the presence of varying concentrations of compound **1** (a), {SbW_9} (c), imi (d) in 298K and compound **1** (b) in 318K. The concentrations of compounds were 0, 1.25, 2.5, 3.75, 5, 6.25, 7.5, 8.75 and 10 μM; pH = 7.4, λex = 280 nm, c (BSA) = 2 μM. (e) The plots of log((F_0-F)/F) vs.log(Q) for compound **1**; (f) Absorption spectra of DNA in the absence and in the present of compound **1**, imi, {SbW_9}. The concentrations of compounds were 2.5 μM; pH = 7.4, c (BSA) = 2 μM.

Table S8. The bingding constants, bingding sites and thermodynamic parameters of the binding interactions of BSA with compound **1**.

	T(K)	K (mol Ł$^{-1}$)	n	$R^{(a)}$	△H ?(KJ/mol)	△G ° (KJ/mol)	△S ° (J/(mol Ł K))
Compound 1	298	4935	0.7919	0.99876	-14.71	-21.069	21.338
	318	3397	0.7189	0.99388		-21.496	